The Identification and Analysis of Long-Range Aerosol Transport Pathways with Layered Cloud-Aerosol Lidar with Orthogonal Polarization Datasets from 2006 to 2016

Lingyu Wang [1,2,3], Wensheng Wang [1,2], Baolei Lyu [4,5,6,*], Jinghua Zhang [1,2], Yilun Han [3], Yuqi Bai [3] and Zhi Guo [1,2]

[1] Key Laboratory of Network Information System Technology (NIST), Institute of Electronics, Chinese Academy of Sciences, Beijing 100190, China
[2] The Aerospace Information Research Institute, Chinese Academy of Sciences, Beijing 100094, China
[3] Department of Earth System Science, Ministry of Education Key Laboratory for Earth System Modeling, Institute for Global Change Studies, Tsinghua University, Beijing 100084, China
[4] Huayun Sounding Meteorology Technology Corporation, Beijing 100081, China
[5] Jiangsu Collaborative Innovation Center of Atmospheric Environment and Equipment Technology (CICAEET), Nanjing University of Information Science & Technology, Nanjing 210044, China
[6] China Meteorological Administration Xiong'an Atmospheric Boundary Layer Key Laboratory, Xiong'an 071000, China
* Correspondence: lvbaolei@hysdqx.com

Contents of this file

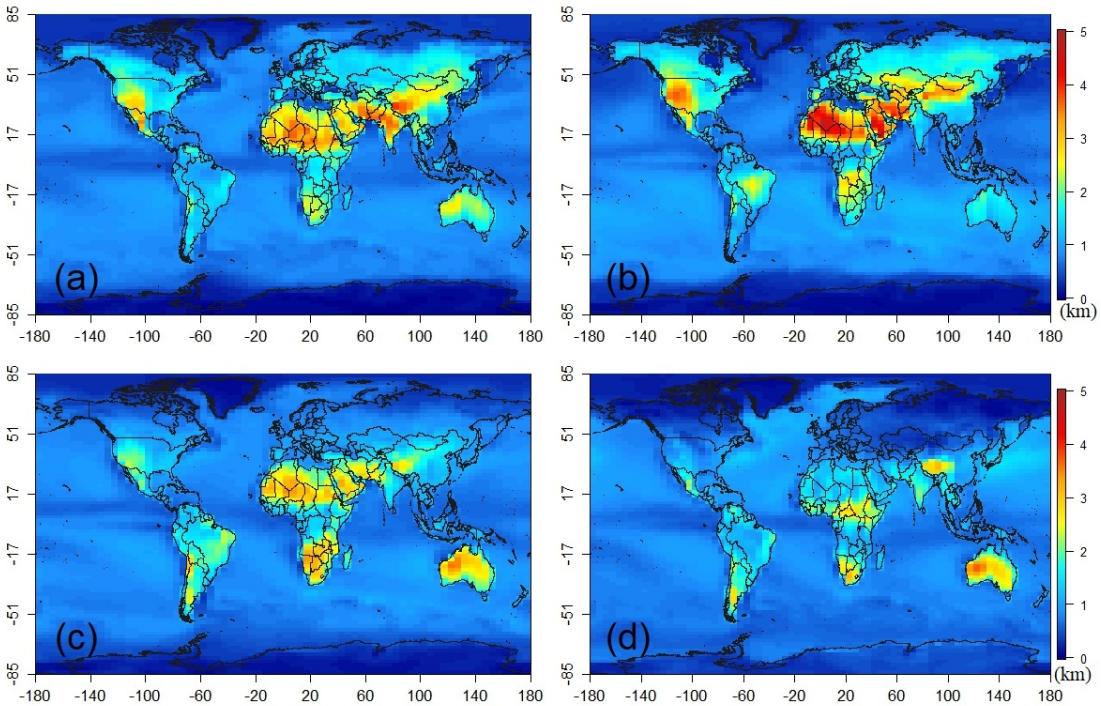

Figure S1. Planetary boundary layer height (PBLH) on the global scale: (a-d) the PBLH values in MAM (March-April-May), JJA (June-July-August), SON (September-October-November) and DJF (December-January-February).

Table S1. The ratios of air mass forward trajectories in each cluster on a seasonal scale (the North China Plain)

clusters	MAM	JJA	SON	DJF
1	36.4%	17%	27.3%	19.3%
2	20.3%	29.45%	26.25%	24.0%
3	37.7%	14.6%	24.5%	23.2%

Table S2. The ratios of air mass forward trajectories in each cluster on a seasonal scale (the Taklimakan Desert)

clusters	MAM	JJA	SON	DJF
1	20%	27.7%	20.4%	31.9%
2	38.9%	9.6%	37.1%	14.4%
3	24.3%	24.1%	26.4%	25.2%

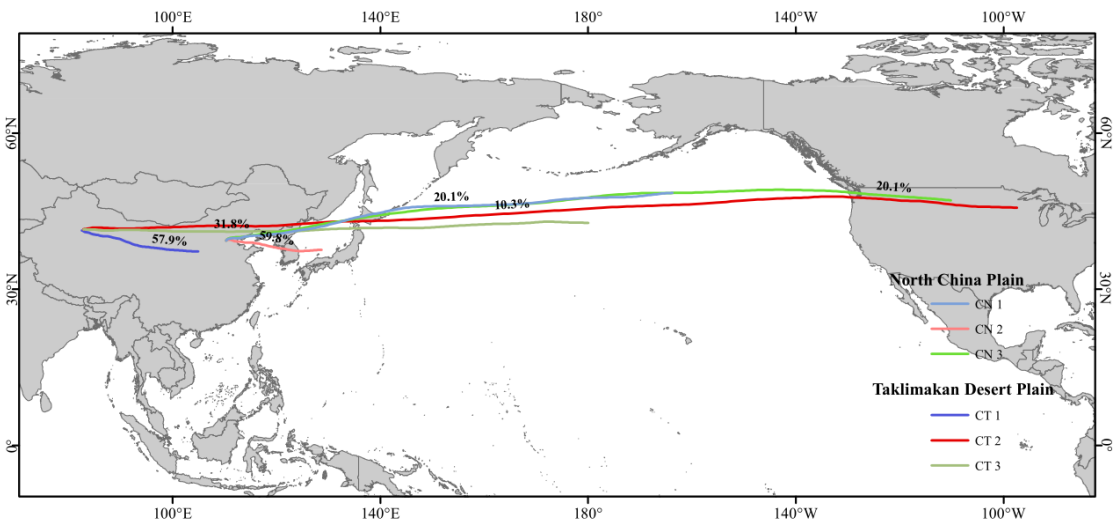

Figure S2. 11-day air mass forward trajectory clusters originating from the North China Plain and the Taklimakan Desert (starting at 500 m AGL).

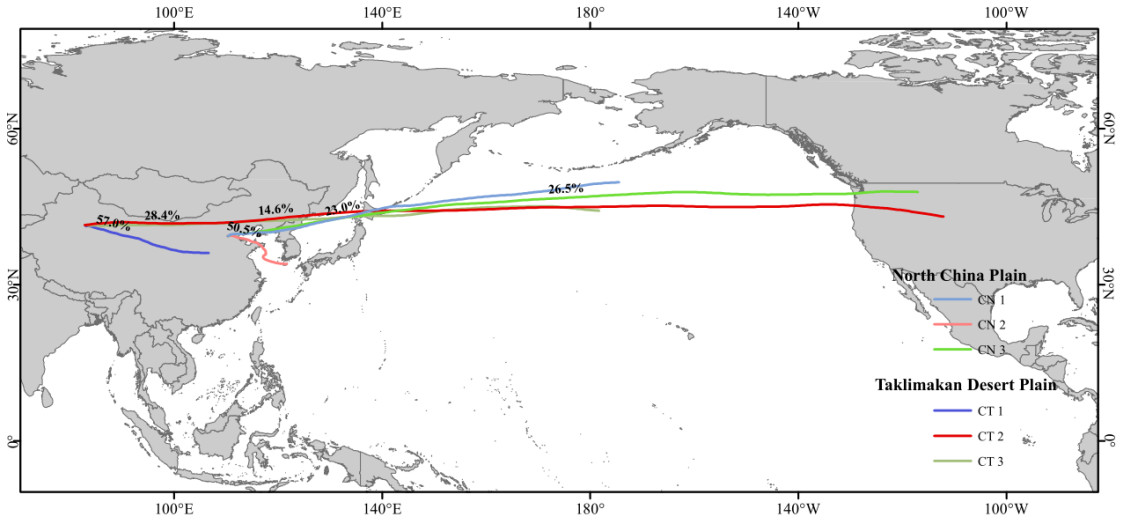

Figure S3. 11-day air mass forward trajectory clusters originating from the North China Plain and the Taklimakan Desert (starting at 1000 m AGL).

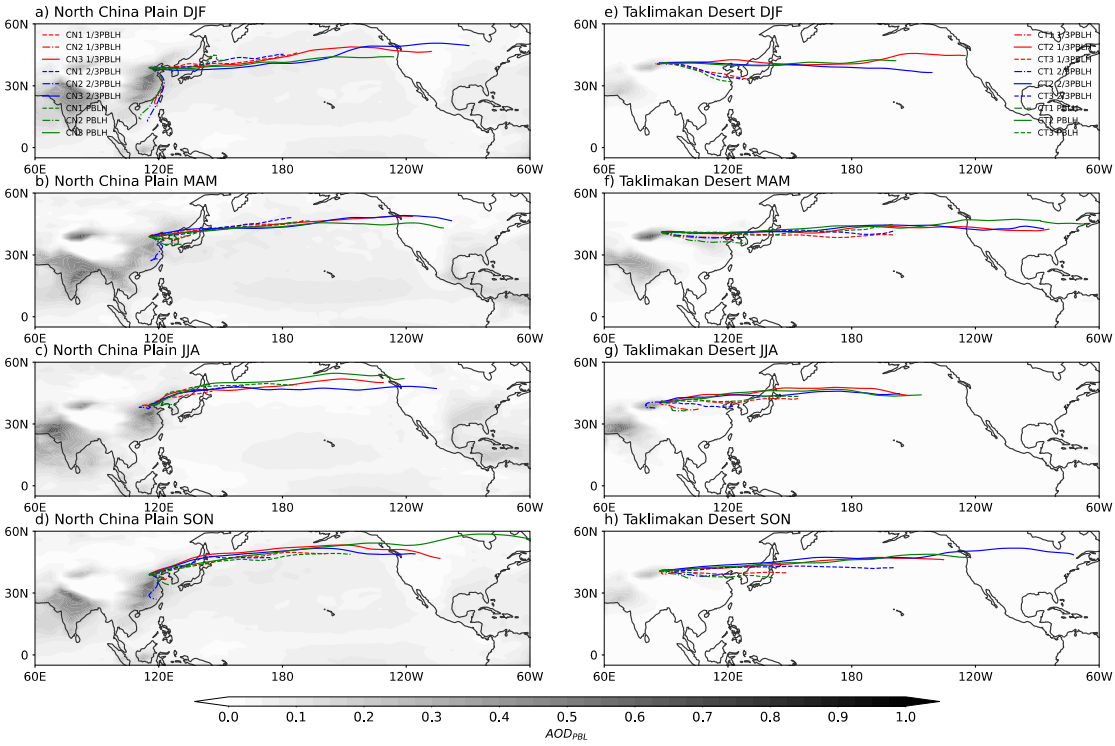

Figure S4. 11-day air mass forward trajectory clusters originating from the North China Plain (a-d) and the Taklimakan Desert (e-h). Started levels are at 1/3PBLH, 2/3PBLH, and PBLH in the air mass forward trajectories calculation. The shades (a-d) are the AOD_{PBL} values of total aerosols, while the shades (e-h) are the AOD_{PBL} values of dust aerosols.

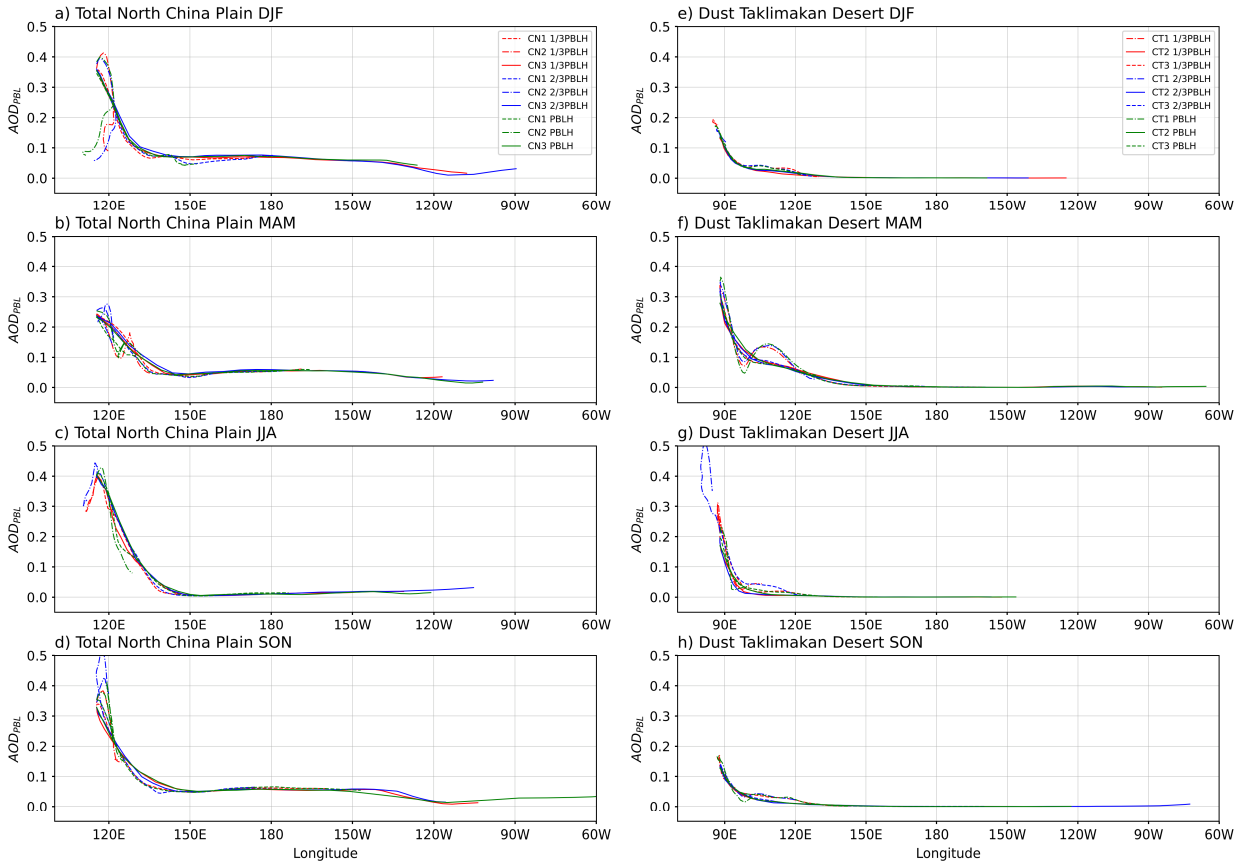

Figure S5. AOD_{PBL} values of total aerosols along air mass forward trajectory clusters originating from the North China Plain (a-d), and AOD_{PBL} values of dust aerosols along air mass forward trajectory clusters originating from the Taklimakan Desert (e-h). Started levels are at 1/3PBLH, 2/3PBLH, and PBLH in the air mass forward trajectories calculation.

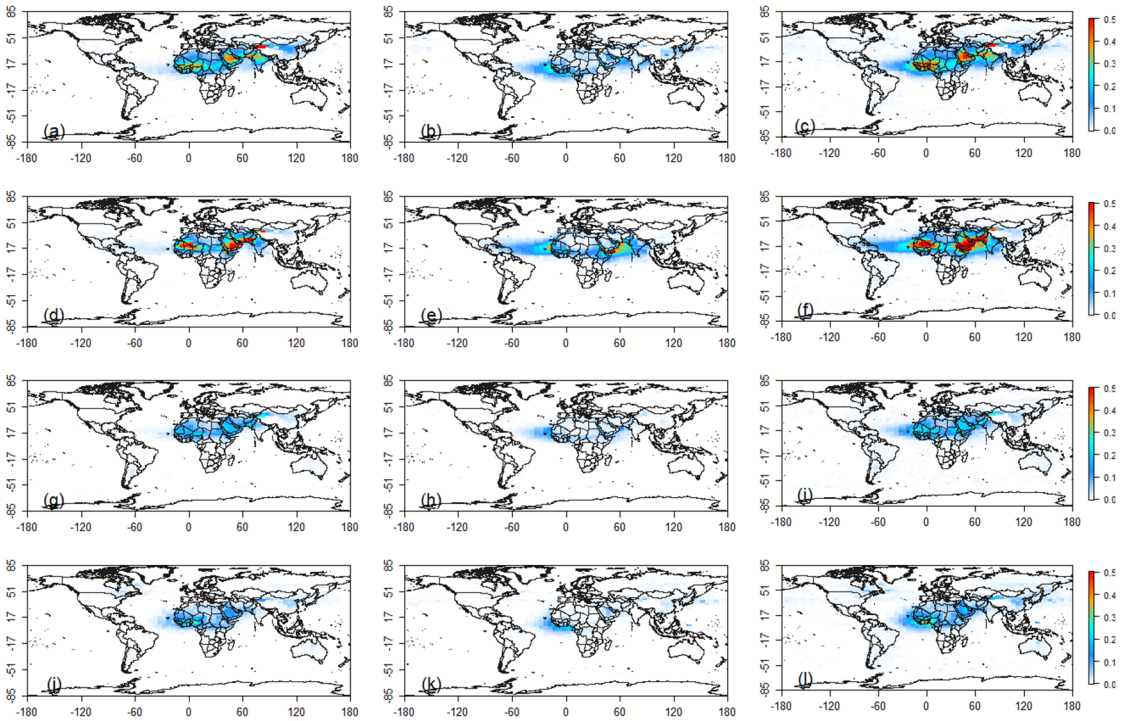

Figure S6. Seasonal layered AOD values for dust. The four rows represent four seasons, which are MAM, JJA, SON, and DJF. The three columns are for AOD_{PBL}, AOD_{FTL}, and AOD_{TA}.

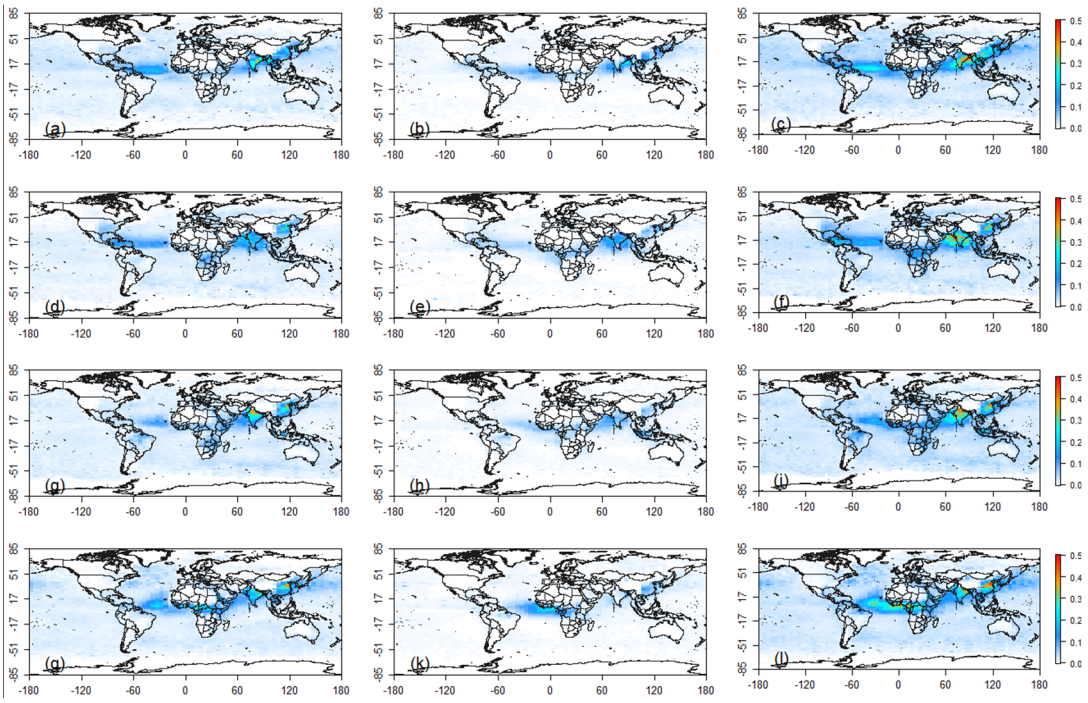

Figure S7. Seasonal layered AOD values for polluted dust aerosols. The four rows represent four seasons, which are MAM, JJA, SON, and DJF. The three columns are for AOD_{PBL}, AOD_{FTL}, and AOD_{TA}.

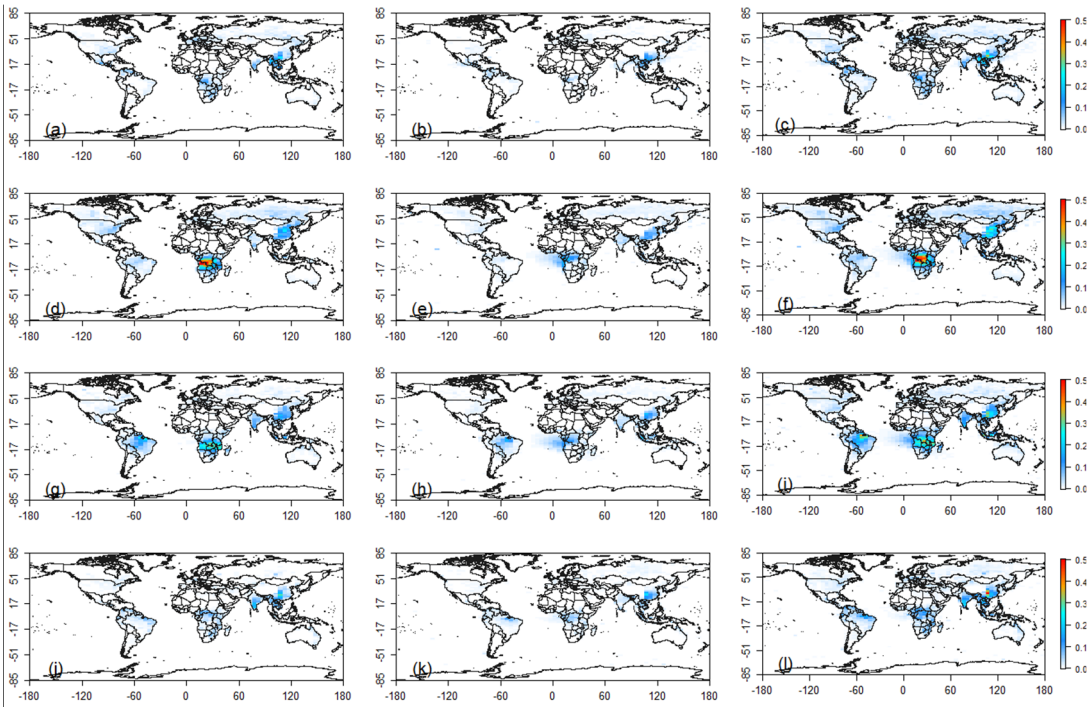

Figure S8. Seasonal layered AOD values for smoke aerosols. The four rows represent four seasons, which are MAM, JJA, SON, and DJF. The three columns are for AOD_{PBL}, AOD_{FTL}, and AOD_{TA}.

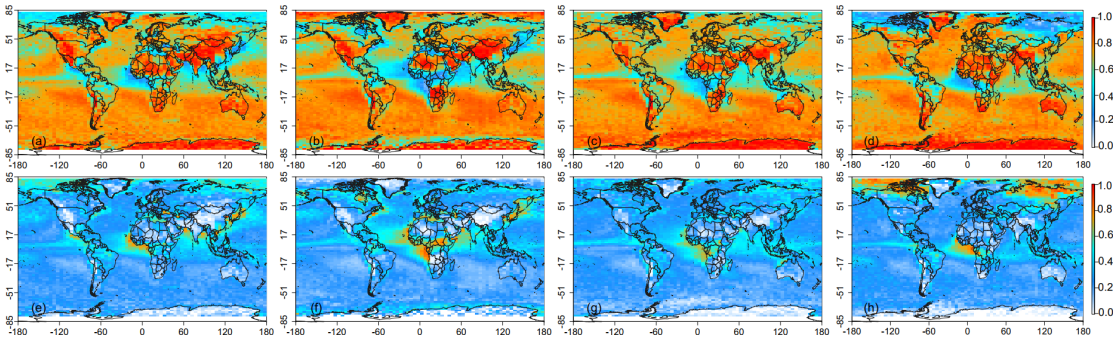

Figure S9. (a-d) R_AOD$_{PBL}$ values and (e-h) R_AOD$_{FTL}$ values in four seasons.

Columns 1-4 correspond to four seasons, which are MAM, JJA, SON, and DJF.

Table S3. Summary of the R_AOD_{PBL} values over the land.

	Mean	Min.	1st Qu.	Median	3rd Qu.	Max.
MAM	74.1	28.7	65.0	75.3	84.8	100.0
JJA	71.6	14.8	62.2	73.1	82.3	100.0
SON	71.6	25.0	62.9	71.2	80.9	100.0
DJF	65.4	8.0	53.0	69.2	80.8	100.0

Table S4. Summary of the R_AOD_{PBL} values over the ocean

	mean	Min.	1st Qu.	median	3rd Qu.	Max.
MAM	71.0	18.9	66.4	74.5	78.3	90.6
JJA	71.3	14.2	65.2	75.5	80.1	90.9
SON	73.1	27.5	69.0	74.9	79.7	96.9
DJF	76.1	13.8	70.6	75.6	79.1	100.0

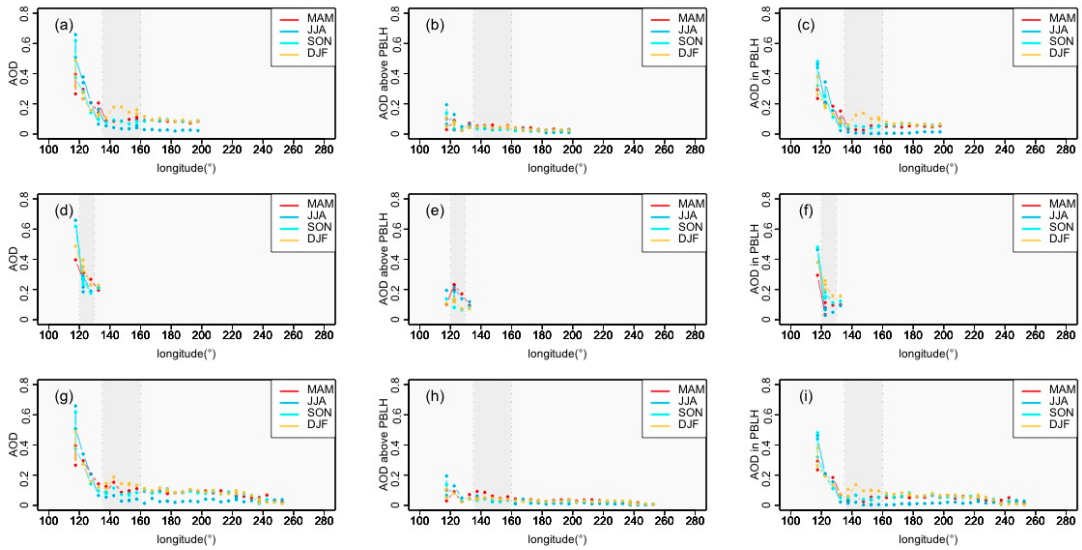

Figure S10. (a, d, g) AOD_{TA}, (b, e, h) AOD_{FTL}, and (c, f, i) AOD_{PBL} along three long-distance aerosol transport pathways (CN1, CN2, and CN3) on a seasonal scale (from the North China Plain).

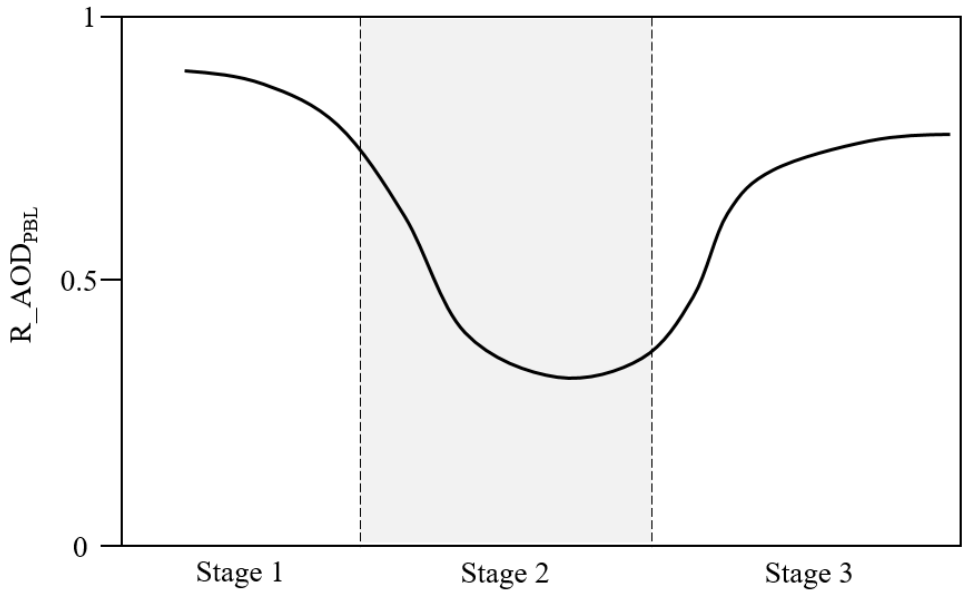

Figure S11. Three-stage conceptual model depicting the changes of R_AOD$_{PBL}$ in long-range aerosol transportation

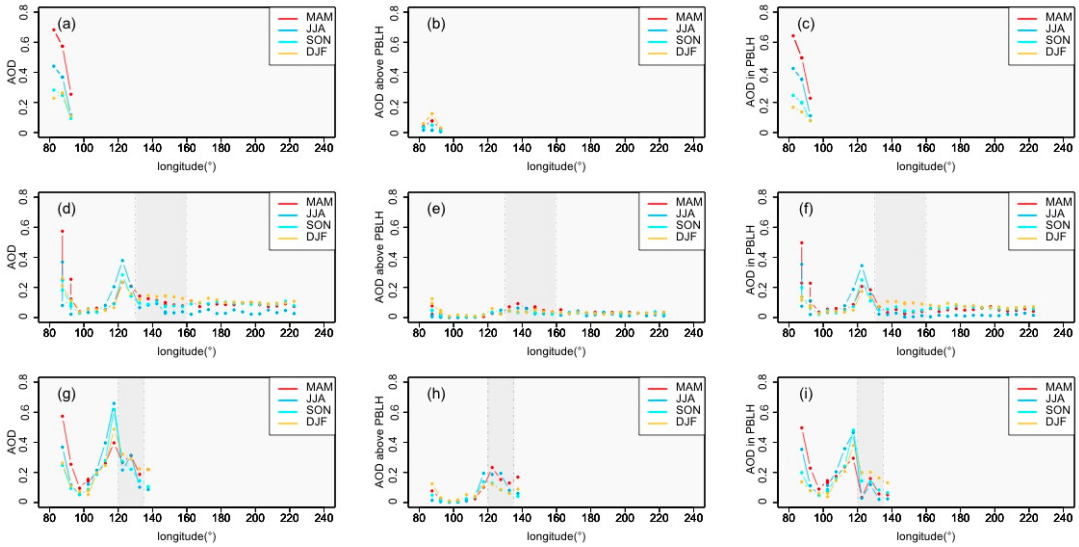

Figure S12. (a, d, g) AOD_{TA}, (b, e, h) AOD_{FTL}, and (c, f, i) AOD_{PBL} along three long-distance aerosol transport pathways on a seasonal scale (from the Taklimakan Desert).